REVIEW OF HIGH SENSITIVITY AC FIELD MEASUREMENT - RECENT ADVANCES AND FUTURE WORK

D. Mirshekar-Syahkal
Department of Electronic Systems Engineering
University of Essex
Colchester, Essex CO4 3SQ, UK

INTRODUCTION

The high sensitivity ac field measurement (ACFM) is a powerful alternative to the conventional eddy current technique. This technique does not require an electronic bridge or a differential probe. It uses a current-carrying rectangular coil or a rhombic loop for producing the eddy current in the work-piece, and a linear probe attached to the inducer in a particular location to sample the field tangent to the metal surface. In this paper, initially a review of the ACFM technique in crack detection and sizing is given. Then the principles behind the high sensitivity ACFM are addressed. Recent advances in this technique, including the development of flat inducers, accurate modelling of field-flaw interaction, and techniques for crack signal inversion, are reported. The application of the technique in detection of cracks using high lift-off probes, shallow cracks, cracks in welded areas and heat affected zones, is highlighted. Also, a linear array system based on the high sensitivity ACFM for detection of defects in large metal surfaces, is discussed. The final part of the paper concerns with future work on the high sensitivity ACFM which is of particular interest in practical NDE.

THE ACFM AND THE HIGH SENSITIVITY ACFM TECHNIQUES

The AC field measurement technique is evolved from the AC potential drop method, mainly for the detection and sizing of surface cracks in metals. In the original ACFM, a uniform thin-skin eddy current is made incident upon the crack, and a vertical or horizontal magnetic probe is used to detect perturbations in the magnetic field above the metal surface, Fig.1.a,. The principles behind the uniform field ACFM and details of the associated field-flaw modelling, are well documented in [1, 2]. In the uniform field ACFM, the field is not affected by the depth of a uniform crack (ie: a crack with infinite aspect ratio) and any signal detected, is mainly due to the crack gape. However, this effect is not a problem in practical cases, where cracks have small aspect ratios, since the magnetic field around such cracks is a function of the crack depth.

In order to overcome the problem of sensitivity to depth for long cracks, particularly when measurements are not carried out near the crack ends, the use of a finite size inducer was considered necessary [3]. Near a crack, the field of such an inducer is a function of the depth. A suitable inducer is a small rectangular coil, and the probe can be a small wire wound coil located below the inducer. The probe can be attached to the inducer in various positions and with different orientations. For example, it can be attached to the inducer with its axis parallel to the axis of the inducer, Fig.1.b [4]. In this position, it behaves as an absolute probe. Crack signals from this probe were found to have very small phase variations, Fig.2.a. It is well-known that absolute probes use up the detector dynamic range in an efficient way. For example, the signal in Fig.2.a was obtained when the detector was close to saturation. However, this problem can be cured by using a differential probe or a bridge system, but the associated electronic circuits add to the complexity of the detector.

Another position of the probe is in the front of the inducer, Fig.1.c. It was found that when a linear coil (in which the number of turns is proportional to the probe length) is used as the probe with its axis normal to the inducer axis, the sensitivity increases significantly

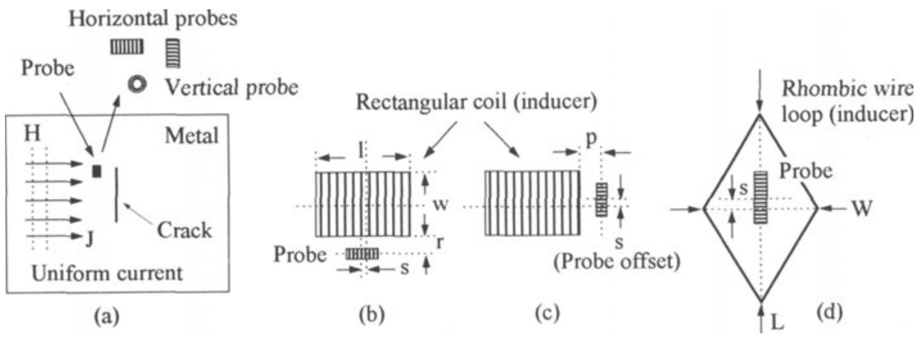

Fig.1 (a) Uniform field ACFM, (b) inducer and probe combination which makes ACFM sensitive to the depth of long cracks, (c) and (d) probe and inducer combinations for high sensitivity ACFM. In this work, for (b) and (c), inducer thickness=4.5 mm, l=10 mm, w=12 mm, p=5 mm and r=1.5 mm and for (d) W=11.3 mm and L=21.5 mm. In (b), (c) and (d), the probes are at a distance of h-q below the inducer where q and h are the probe and inducer lift-offs respectively. Figures are in plan-view.

compared to the previous case [4]. For example, our system showed about 30 dB sensitivity enhancement. Such a sensitivity enhancement can be achieved if the probe is symmetrically (or nearly symmetrically) located with respect to the inducer axis. In Fig.2.b, the crack signal corresponding to this position of the probe are shown. In contrast to the phase in Fig.2.a, a large phase change is apparent in the signal in Fig.2.b and the detector is far from saturation. The value of the phase was found to be dependent on the crack depth and the probe offset [4, 5]. However, the maximum phase change is 180° and that occurs when the probe is balanced. In the new position, which is called the null field position, the probe is subjected to two equal, but opposite field components, thus behaving like a differential probe [4]. This allows efficient use of the detector dynamic range, and is one reason for increased sensitivity. But more importantly, it was found that the phase of the field component along the probe axis, on either side of the null field, is affected by the crack depth and this has a constructive contribution to the sensitivity. The new probe-inducer does not require a bridge in the detection, which is of particular advantage in applications like probe arrays, since the detector circuit is substantially simplified and no tuning is required. The ACFM using a linear probe at the null field is known as the high sensitivity ACFM.

The rectangular coil is not the only inducer with the favourable null field. The rhombic inducer, Fig.1.d, also benefits from this property. It is basically a current carrying rhombic wire loop, and if required, can be printed on a thin flexible printed circuit board. The probe is fixed below the inducer with its axis along the long diagonal. The probe length is normally shorter than the diagonal.

The rhombic inducer and the probe shown in Fig.1.d were used to detect very shallow surface cracks (as small as 50 μm in depth) in mild steel and aluminum [6]. Also, with this probe-inducer, experiments showed that a 0.5 mm deep notch in mild steel can be detected at a probe lift-off of about 8 mm, Fig.3.a. In this case, the phase variation is found to be significantly smaller than that associated with the signal obtained close to the metal surface, Fig.3.b. This effect can be attributed to the combination of a common-mode voltage greater than the signal, and an inevitable residual probe offset. Nonetheless, the results indicate that a metal covered with a thick plastic material or paint can be inspected by the high sensitivity ACFM. Furthermore, it was shown that this technique can reliably detect heat affected zones, ground welds and generally, regions with different conductivities [7]. Of particular interest is the detection of cracks in welded regions. It was found that in such applications, a long linear probe is needed in order to enhance the crack signal while averaging out the background noise due to surface irregularities [6].

MATHEMATICAL MODELLING

An accurate mathematical method was developed for the interaction of the field of an arbitrary inducer with a long uniform crack. Details of the technique are presented in [8]. It benefits from three features: (i) It includes a new boundary condition [2] at the metal-air interface (coinciding with the xy plane), given by

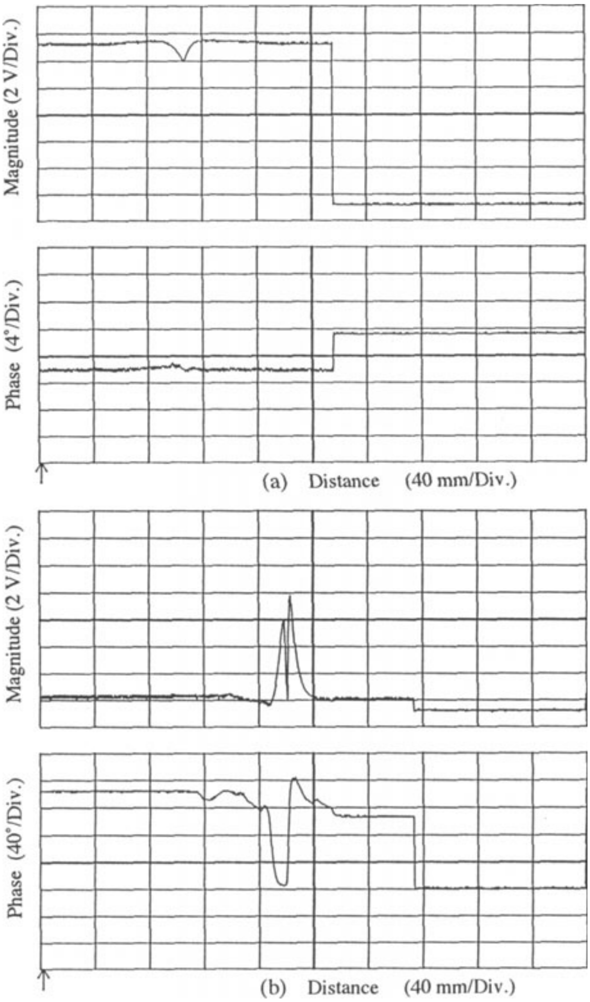

Fig.2 Signals from the scans of a long closed (invisible) fatigue crack in mild steel, (a) with the probe-inducer in Fig.1.b and (b) with the probe-inducer in Fig.1.c; q=0.76 mm, h=3.91 mm, s≈0 mm, probe length=4 mm, probe core diameter=0.88 mm, no. of probe turns=80, layers of windings=2, wire diameter=0.0032" and f=20 kHz.

$$\frac{\mu}{k}\nabla_t^2\psi + \mu_0 \frac{\partial\psi}{\partial z} = -\left(\frac{2\mu}{k} + \mu_0 g\right)H_z(x,0)\delta(y) \qquad \left(k = \sqrt{j\omega\mu_0\mu_r\sigma}\right) \tag{1}$$

This boundary condition is suitable for both ferromagnetic and non-ferromagnetic metals and is based on the assumption of thin-skin current. It also includes the effect of the crack opening (g). In (1), ψ is the sum of the scattered and incident field potentials ($\psi = \psi_i + \psi_s$), $H_z(x,0)$ is the normal component of the magnetic field distribution at the crack mouth just inside the crack (at z=0) and other parameters have their usual meaning. (ii) The technique is analytical-numerical and is based on the fast Fourier transform, leading to high computational efficiency. In fact, the two-dimensional (2-D) Fourier transform (FT) was employed to convert (1) to an algebraic form, allowing one to obtain the final solution in the Fourier domain. (iii) The technique can handle arbitrary shape current carrying conductors and employs scalar potentials. The conductor is divided into current elements and for each element a Fourier domain scalar magnetic potential is defined in terms of the Fourier domain vector magnetic potential of the element.

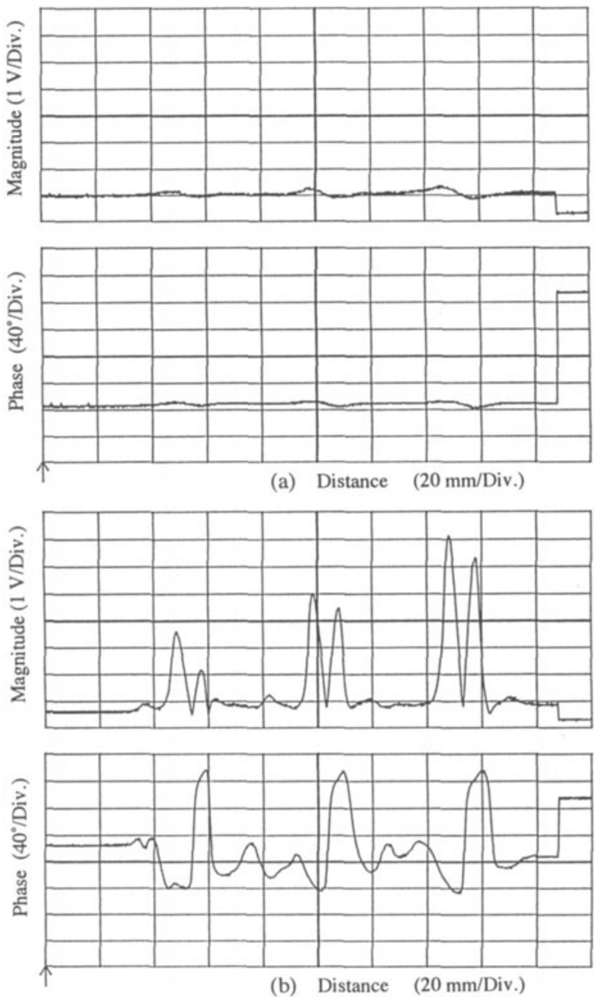

Fig.3 Signals from the scans of 0.5, 1 and 2 mm deep fine saw-cut notches (of opening g=0.15 mm) in mild steel with the probe-inducer in Fig.1.d for two probe lift-offs, (a) q≈8 mm and (b) q≈0.76 mm; h-q=2.4 mm and f=20 kHz. The probe is 13.5 mm long, has 260 turns and an offset s≈0 mm, otherwise it is the same as that in Fig.2.

The final solution in the Fourier domain is given by

$$\tilde{\tilde{\psi}}(z) = \tilde{\tilde{\psi}}_i(0)\, e^{\gamma z} + \left(\frac{1-\frac{\mu_r}{k}\gamma}{1+\frac{\mu_r}{k}\gamma}\right)\tilde{\tilde{\psi}}_i(0)\, e^{-\gamma z} + \frac{\left(\frac{2\mu_r}{k}+g\right)}{\gamma\left(1+\frac{\mu_r}{k}\gamma\right)}\tilde{H}_z(\alpha,0)\, e^{-\gamma z} \tag{2}$$

where $\gamma = \sqrt{\alpha^2+\beta^2}$ with α and β being the spectral parameters of the 2-D FT (≈) and $\tilde{\tilde{\psi}}_i(0)$ is the spectral domain form of the incident field potential at the metal surface. In (2), the second and third terms on the right hand-side are the scattered field potentials due to the metal and the crack respectively and the 1-D FT (~) of $H_z(x,0)$ is given by

$$\tilde{H}_z(\alpha,0) = -2\alpha\tanh(\alpha d)\int_{-\infty}^{+\infty}\frac{\tilde{\tilde{\psi}}_i(0)}{1+\frac{\mu_r}{k}\gamma}d\beta \Big/ \left[\sqrt{2\pi} + \left(\frac{2\mu_r}{k}+g\right)\alpha\tanh(\alpha d)\int_{-\infty}^{+\infty}\frac{d\beta}{\gamma\left(1+\frac{\mu_r}{k}\gamma\right)}\right] \tag{3}$$

where d is the crack depth.

Based on the formulation, a computer program was developed which can deal with the interaction of the fields of the rectangular and rhombic inducers with long cracks. It can simulate the field and the crack signal. Examples and comparisons with measurements are given in [8]. Of particular interest in this paper is the predication of the effects of different probe offsets, s, on the crack signal. This is shown in Fig.4 for a 4 mm deep notch in mild steel. For a nearly balanced probe (s=-0.2 mm), the magnitude exhibits two almost equal peaks and a large phase change. As the offset increases, the difference between the two peaks increases, the phase change decreases and the distance over which the phase changes, reduces. For large offsets, one of the two peaks converts to a trough and the phase change becomes very small. In Fig.4, the signal for a 4 mm notch in aluminum for s=-1.5 mm, is also shown. Note that it is vastly different from its counterpart for steel.

INVERSION TECHNIQUES

Two techniques for the inversion of the crack signal associated with the high sensitivity ACFM, were developed. Both are appropriate for long cracks. One of these is based on theoretical data, which is similar to the inversion procedure in [9]. In this technique, curves obtained by the computer program (mentioned in the previous section), relating crack depth to (Vp-Vr)/Vr (where Vp is the major peak in the crack signal and Vr is the voltage in the absence of crack, Fig.4), are used to determine the crack depth from the signal. Fig.5.a shows a set of such curves for a rhombic inducer employing a linear probe for application to mild steel. In this inversion technique, the probe is set to have some offset ($s \neq 0$), leading to $Vr \neq 0$ for the purpose of normalizing. If the probe offset is not known, it can be estimated from the ratio of the two peaks (or the peak and the trough) in the crack signal, using a curve which can also be produced by the computer program. A careful examination of crack signals (eg: Fig.4) reveals that a peak (or a trough) occurs when one end of the probe is just over the crack.

The second technique is experimental and involves the measurement of Vp-Vr for crack and for a set of fine saw-cut notches with known depths. The results are compared to find the crack depth at different locations. In this technique, the current to the inducer has to be maintained the same in the calibration and crack detection process. The chief advantage of using Vp-Vr is its low sensitivity to variations in the probe offset, s. For example, Fig.5.b shows that even a large error of 1 mm in s (from the balanced position) produces only about 10% variation in Vp-Vr. Therefore, in inversions involving an array with probes having similar (but not exact) offset values, the crack signal (which is the combination of Vp-Vr of all probes) is a good representative of the crack profile. Examples of this inversion technique are presented in the following section. In Fig.5.b, the normalization parameter is the input current to the inducer which is assumed to be 1 A.

ARRAY

The high sensitivity probe-inducer employing the rhombic wire loop, Fig.1.d, can be exploited in order to develop flexible linear probe arrays, Fig.6 [10]. The consecutive inducers

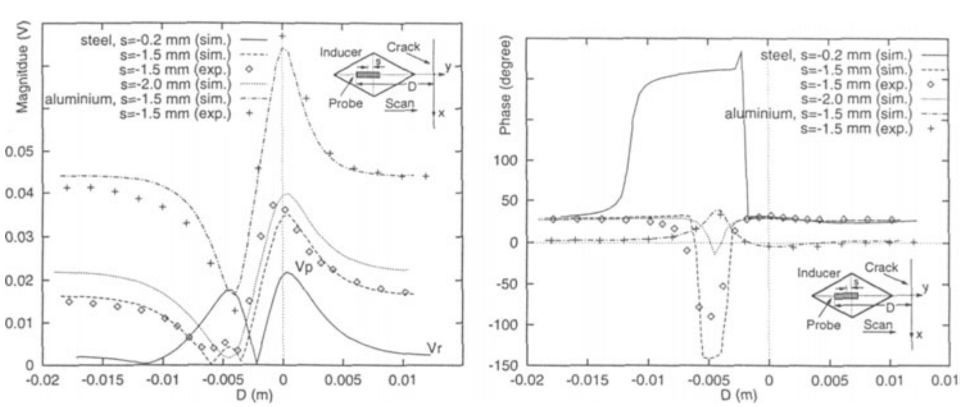

Fig.4 Theoretical and measured signals for various probe offsets, s, associated with the scan of a 4 mm notch in mild steel and aluminum with the probe-inducer in Fig.1.d. The probe is the same as that in Fig.2; h-q=2.4 mm, q=0.76 mm and f=20 kHz. Notch opening g=0.15 mm in steel and g=0.25 mm in aluminum.

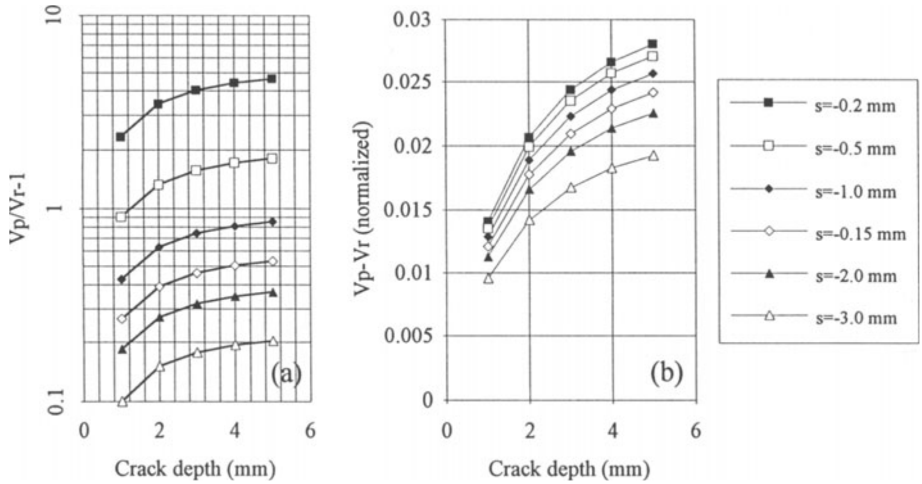

Fig.5 Curves for inverting crack signals obtained from the scans of long uniform cracks in mild steel with the probe-inducer in Fig.1.d. The probe specifications and the probe and inducer lift-offs are the same as those in Fig.7.

in a linear array must have opposite currents, otherwise the resultant field tends to be uniform, giving rise to very weak interaction between the field and long cracks. A further problem is the signal saturation associated with the probe-inducer in Fig.1.d. This effect which is well-known in eddy current techniques [11], can be reduced by increasing the spacing between the inducer and the probe [12]. This is, of course, achieved at the expense of the reduction of the probe density (number of probes/unit length).

Details of a prototype array similar in structure to Fig.6 is in [10], together with its switching system. The array is sufficiently flexible for applications on curved surfaces with a radius of curvature greater than 50 cm. Arrays for tighter curvatures can be easily fabricated using surface mount electronic components. The prototype array consists of 28 units (including 28 probes) and is about 28 cm long. It can cover an area of about 28 x 2 cm^2. In principle, the array can be made arbitrarily long, but, as explained in [10], its special sequential switching system imposes a length limit. Calculation shows that using suitable silicon transistors, switching systems with 200 transistors would be feasible. This corresponds to an array of about 2 m length with a probe spacing of 10 mm.

The prototype array was evaluated on mild steel and aluminum containing fatigue cracks and fine saw-cut notches. Reliable and consistent signals were always obtained. Example signals from a shallow arc-circular notch with a small opening, simulating a crack in aluminum, is shown in Fig.7 and from an invisible fatigue crack in mild steel in Fig.8. In Fig.8, there are also signals corresponding to the application of the array to a set of saw-cut notches of uniform

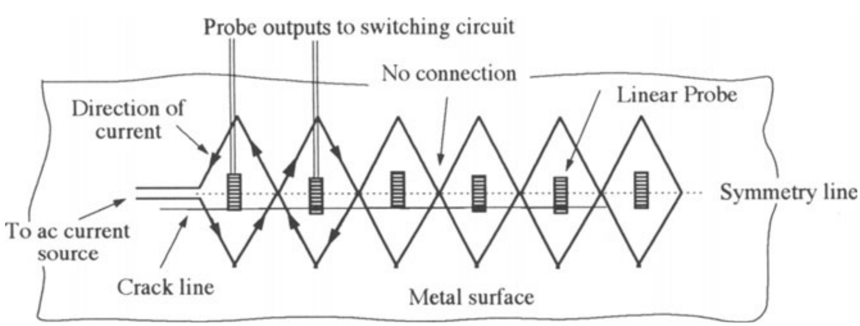

Fig.6 The schematic diagram of a linear array using the rhombic inducer and the linear probe in Fig.1.d, including the direction of the current in the inducers and the array orientation with respect to a crack for the signal inversion.

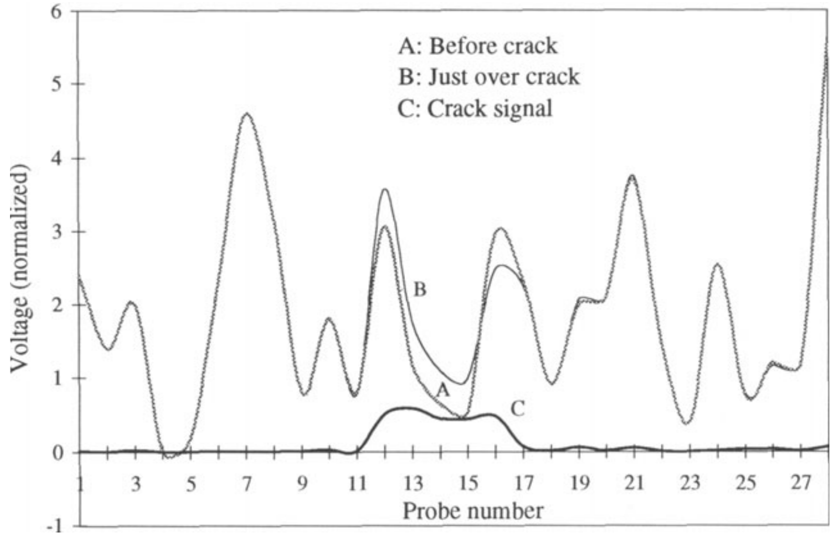

Fig.7 Signals, including the crack signal (C=|Vp-Vr| where Vr=A and Vp=B), from the application of the prototype array to a simulated crack with 51 mm length, 0.5 mm depth and 0.1 mm opening in aluminum at f=20 kHz. Each inducer in the array is the same as that in Fig.1.d and probe specifications are: probe length=10 mm, probe core diameter=1.18 mm, no. of probe turns=200, layers of windings=2, wire diameter=0.0032", h-q=2.25 mm and q=0.83 mm.

depth ranging from 0.5 mm to 4 mm with 150 μm opening and to an arc-circular notch with a length of 36 mm, maximum depth of 5 mm and opening of 150 μm. These signals were produced using |Vp-Vr| where Vp and Vr are shown in Fig.4. The signals should approximately represent the profiles of the crack and notches .

The results in Figs.7 and 8, indicate the high potential of the array in detection of shallow and deep cracks with finite and infinite aspect ratios in ferrous and non-ferrous metals. As far as the inversion is concerned, for uniform or nearly uniform cracks, the two inversion techniques mentioned earlier, can be used. However, the main problem with the first technique is the determination of the probe offsets due to the large number of probes involved in the array. In this case, the second inversion approach based on the calibration is preferred. For example, results A to E in Fig.8 which is produced using the difference |Vp-Vr|, can act as calibration curves for the array. In spite of the large probe offsets involved, the results show the uniformity of the depths of the notches within a 20% error bound. This was expected in view of small sensitivity of |Vp-Vr| to a large change in the probe offset, as mentioned earlier in the inversion section. Using the calibration curves, the depth of the arc-circular notch producing signal G in Fig.8, is estimated to be about 4 mm which is 1 mm less than its exact value. The underestimation is due to the effect of the crack length, which is not accounted for in the inversion process.

CONCLUSION AND FUTURE WORK

The high sensitivity AC field measurement (ACFM) technique, has proved to be highly successful in detecting closed/open surface cracks with finite and infinite aspect ratios in ferrous and non-ferrous metals. With this technique, we detected cracks as small as 50 μm in depth in mild steel and aluminum, picked up a 1 mm deep crack in a roughly welded mild steel [6] and revealed a 0.5 mm deep crack in a mild steel block covered by an 8 mm thick layer of a non-metallic material, Fig.3.a.

So far, the experimental and theoretical work on the high sensitivity ACFM has been mostly concentrated on long uniform cracks under laboratory condition. The simulation and inversion of crack signals are based on an accurate one-dimensional field-flaw modelling [8]. In practice, crack length, gape and bridging (lines or points of contact), oxidisation, variation in metal properties (eg: due to heat effects), surface finish (especially in welded areas) and geometry of the component under test, affect the crack signal, hence giving rise to some errors

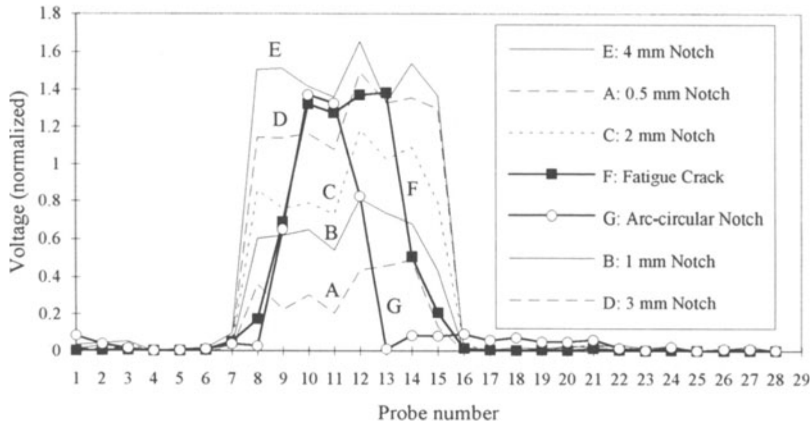

Fig.8 Signals from the application of the prototype array (specified in Fig.7) to a set of fine saw-cut notches (A to E), to a closed (invisible) fatigue crack (F) and to an arc-circular notch (G) at 20 kHz.

in the predication of the crack type and the crack depth from the developed modelling. Therefore the future work on the high sensitivity ACFM for practical NDE is (i) to recognise and quantify the effects of various geometrical and metal parameters (mentioned above) on the crack signal and on the crack depth measurement when using the one-dimensional modelling, (ii) to extend and improve the accuracy of the modelling, directly accounting for the effects of some of the significant geometrical parameters including crack length and bridging, and (iii) to develop simple methods for accurate sizing of the crack depth. Some work has already been carried out on the effects of the crack length on the crack signal [13].

ACKNOWLEDGEMENT

Part of this work was supported by the EPSRC of the UK under research grant GR/J50972.

REFERENCES

1. A. M. Lewis, D. H. Michael, M. C. Lugg and R. Collins, J. of Appl. Phys., 64, (1988), p. 3777.
2. D. H. Michael, A. M. Lewis, M. McIver and R. Collins, Proc. R. Soc. Lond., A434, (1991), p. 587.
3. S. H. H. Sadeghi and D. Mirshekar-Syahkal, in *Review of Progress in QNDE*, Vol. 9A, eds. D. O. Thompson and D. E. Chimenti (Plenum Press, New York, 1990), p. 351.
4. D. Mirshekar-Syahkal, C. Moschovinos and P. Hadjikyriakos, in *Review of Progress in QNDE*, Vol. 13A, *op. cit.*, (1994), p. 1095.
5. D. Mirshekar-Syahkal, *Proc. of the 3rd Int. Conf. on Computation in Electromagnetics*, IEE Publ., no. 420, (1996), p. 133.
6. D. Mirshekar-Syahkal and R. F. Mostafavi, in *Review of Progress in QNDE*, Vol. 15A, *op. cit.*, (1996), p. 1121.
7. R. F. Mostafavi and D. Mirshekar-Syahkal, IEEE Trans. Magn., 33, (1997), to appear.
8. D. Mirshekar-Syahkal and R. F. Mostafavi, IEEE Trans. Magn., 33, (1997), p. 2291.
9. S. H. H. Sadeghi, and D. Mirshekar-Syahkal, in *Review of Progress in QNDE*, Vol. 14A, *op. cit.*, (1995), p. 275.
10. R. F. Mostafavi and D. Mirshekar-Syahkal, in *Review of Progress in QNDE*, Vol. 16A, *op. cit.*, (1997), p. 1029.
11. V. S. Cecco and G. Van Drunen, in *Research Techniques in Nondestructive Testing*, Vol. 8, ed. R.S. Sharp (Academic Press: London, 1985), p. 269.
12. D. Mirshekar-Syahkal and R. F. Mostafavi, in *Review of Progress in QNDE*, Vol. 16B, *op. cit.*, (1997), p. 1923.
13. R. F. Mostafavi and D. Mirshekar-Syahkal, in *Review of Progress in QNDE*, Vol.17, *op. cit.*, (1998).